Study of oxygen isotopes and $N = 8$ isotones with an extended cluster-orbital shell model

H. Masui*
Information Processing Center, Kitami Institute of Technology, Kitami 090-8507, Japan

K. Katō
Division of Physics, Graduate School of Science, Hokkaido University, Sapporo 060-0810, Japan

K. Ikeda
The Institute of Physical and Chemical Research (RIKEN), Wako 351-0198, Japan
(Received 1 October 2005; published 28 March 2006)

We attempt to obtain a unified description of the bound and unbound states of multivalence nucleons of a core system in the framework of the cluster-orbital shell model (COSM). In this framework, the interaction between the core and a valence nucleon (the core-N interaction) is treated microscopically, and the changes in both the core structure and the core-N interaction are discussed on the same basis. Furthermore, the center-of-mass motion of every nucleon is completely eliminated, and higher shell configurations, including unbound continuum components, are appropriately taken into account by applying a stochastic variational approach. To examine the reliability of this approach and to discuss how the dynamics of the core reflects to the total system, we study oxygen isotopes and $N = 8$ isotones, which are described by $^{16}\mathrm{O} + Xn$ and $^{16}\mathrm{O} + Xp$ models, respectively.

DOI: 10.1103/PhysRevC.73.034318 PACS number(s): 21.10.−k, 21.60.−n

I. INTRODUCTION

Recent developments in the investigations of unstable nuclei have broadened nuclear physics. Many interesting phenomena, such as halo structures, changes in the magic number, and inversions of single-particle orbits [1–8] have been observed near the drip-line nuclei. To understand such new phenomena, various theoretical studies, from few-body to mean-field approaches, have been carried out. Remarkable developments in the treatment of weakly bound systems have been reported. Explicit investigations of unbound states in many-body systems, including resonant states, can be carried out by extending the variables (coordinates and momenta) to the complex plane [9–11]. However, we are yet to obtain the objective of completely understanding the phenomena of drip-line nuclei.

Large-scale shell-model calculations for bound states [12–14] have been performed by using powerful computational facilities. In the shell-model framework, the inclusion of the continua of the single-particle wave functions has been discussed in studies of the continuum shell model [15–17] and the shell model embedded in the continuum [18]. Recently, the Gamow shell-model (GSM) approach [19–25] was developed. In GSM, the resonant single-particle states are included in the model space as the Gamow resonant states [26], and the single-particle basis sets are constructed by using the Berggren completeness relation [27,28]. A remarkable development in the GSM approach is that components of two-particle unbound states can be considered in the framework; however, these components are not yet treated in the continuum shell model and the shell model embedded in the continuum. GSM have been applied for solving many-particle systems such as $^{4}\mathrm{He} + XN$ and $^{16}\mathrm{O} + Xn$ systems [19–21,25]. However, the GSM still contains problems that are yet to be solved, such as the treatment of the center-of-mass motion and the rapid increase in the model space for applications to a large number of valence nucleons [21].

The cluster-orbital shell model (COSM) was originally proposed to study the helium isotopes in the $^{4}\mathrm{He} + \mathrm{X}n$ model space [29]. The binding energies and rms radii of ^{6}He and ^{8}He were studied. COSM combines the advantages of the cluster model and shell-model approaches. From the viewpoint of the cluster model approach, the spurious center-of-mass motion is entirely eliminated, and the asymptotic behavior of the relative motions between the core and valence nucleons are appropriately taken into account. However, from the viewpoint of the shell model, the mean-field correlations among valence nucleons are described with the characteristic coordinate system. Although the importance of nucleon-nucleon correlations among the valence nucleons is clarified and has been studied in the frame work of the extended cluster model (ECM) [30], it is shown that COSM calculations with a large model space can yield a good approximation of the description of such the correlations [31]. Further, the correlations of nucleons in the core, such as pairing [32] and tensor correlations [33], are translated into the couple-channel approach in the COSM formalism. If sufficiently large channels are included in the model space, the coupled-channel approach of COSM will correspond to the mean-field approach.

To study the structures of drip-line nuclei, it is necessary to treat resonant states in the same framework as that for solving the bound states. The complex scaling method (CSM) [9–11], for studying many-particle resonant states, has been applied to the COSM formalism [31–34]. Aoyama *et al*. [31] studied the resonant states of ^{6}He by the detailed application of CSM; they showed that three-body resonances are successfully described in the complex-scaled COSM formalism. Furthermore, a

*Electronic address: hgmasui@mail.kitami-it.ac.jp

comparison between COSM and GSM is performed, and their correspondence and differences in helium and oxygen isotopes are discussed [35].

From the experiments for drip-line nuclei, ^{23}O and ^{24}O are suggested to be candidates of halo nuclei of a particular nature [3,4]. In comparison to typical and light halo nuclei such as ^{6}He, ^{11}Be, and ^{11}Li, the binding energies of ^{23}O and ^{24}O are not so very low; however, their rms radii are large. An experiment analyzed by the Glauber theory suggests that the modification of the ^{22}O core is extendable to ^{23}O [4]. This suggestion indicates that the picture of a single neutron moving around the inert ^{22}O core is no longer valid for ^{23}O. Hence, it can be considered that the structure of ^{23}O with a large rms radius arises not only because of the broad wave function of a valence neutron but also because of a particular change in the dynamics of many nucleons in ^{23}O and ^{22}O.

An abrupt increase in the rms radii is also observed in $N = 8$ isotones (^{16}O + Xp systems) [2]. At $X = 2$, i.e., the ^{18}Ne nucleus, the rms radius is determined to be considerably greater than that of ^{18}O (^{16}O + $2n$ system). Although it is unclear whether ^{18}Ne is a halo nucleus because of the large error bars of the experiment, the radius of ^{20}Mg, the subsequent $N = 8$ isotone, is determined to be very large when compared to that of ^{20}O within small experimental error bars [2].

If we consider a normal configuration of the shell-model picture for the oxygen isotopes, the main component of the valence nucleons is the $0d_{5/2}$ orbit, and the $1s_{1/2}$ orbit will be occupied in the case of ^{23}O. However, in the $N = 8$ isotones, the Thomas-Ehrman shift occurs in the core-p subsystem, on account of the presence of the Coulomb repulsion between the core and valence protons, and the energy difference between the $0d_{5/2}$ and $1s_{1/2}$ orbits decreases. Hence, the component of the $1s_{1/2}$ orbit increases when compared to that of the oxygen isotopes. The change in the components of the valence nucleons affects the rms radii of isotopes and isotones. Therefore, we can expect that the study of $N = 8$ isotones will provide important information on the abrupt increase in the rms radius of the oxygen isotopes.

In this article, we extend the COSM formalism to two areas and study the oxygen isotopes and $N = 8$ isotones. First, we attempt to study to employ a large model space for the valence nucleons. Second, we consider the core dynamics. As a first step toward accounting for the dynamics, we change the core-size parameter, because we consider it to be an important degree of freedom for describing the core dynamics. In the COSM formalism, the interaction between the core and a valence nucleon is constructed microscopically. It is derived from a nucleon-nucleon interaction by folding the core density. The core dynamics reflect the interaction within the folding process. Hence, we can discuss the dynamics of the total system from a microscopic viewpoint through the change in the core-size parameter. This approach will be crucial for discussing the mechanism for the difference in the oxygen isotopes and $N = 8$ isotones as well as the abrupt increase in the rms radii of ^{23}O and ^{24}O.

In Sec. II, we describe the formalism of an extended cluster-orbital shell model and a calculational method for the variational stochastic approach. The calculated results for oxygen isotopes and $N = 8$ isotones are given in Sec. III. The summary and discussions are given in Sec. IV.

II. EXTENDED CLUSTER-ORBITAL SHELL MODEL AND A STOCHASTIC VARIATIONAL APPROACH

In COSM [29], the interaction between the core and a valence nucleon (a core-N interaction) is microscopically constructed from a nucleon-nucleon interaction by folding the core density. In this study, we extend the COSM formalism. Because the core-N potential depends on the structure of the core wave function, the change in the core affects the folded core-N potential. The energy of the total system is determined by the optimum value of the core-size parameter in the sum of the energies of the core and valence nucleons. Therefore, a change in the optimum core-size value affects the properties of the total system, e.g., the rms radius. Hereafter, we refer to this extended COSM as neo-COSM.

A. Formalism of the extended cluster-orbital shell model

We briefly explain the COSM formalism [29]. The total Hamiltonian from which the center-of-mass motion is subtracted is the sum of the core part ($\hat{H}_C$) and the valence nucleons, and it is expressed as follows:

$$\begin{aligned}\hat{H} &= \sum_{i=1}^{A} \hat{t}_i - \hat{T}_G + \sum_{i<j}^{A} \hat{v}_{ij} \\ &= \hat{H}_C + \sum_{i\in V} \hat{t}'_i + \sum_{\substack{m\in C \\ i\in V}} \hat{v}_{im} + \sum_{i<j\in V} (\hat{T}_{ij} + \hat{v}_{ij}). \end{aligned} \quad (1)$$

Here, A is the mass number of the total system. In Eq. (1) C and V represent the nucleons in the core and the valence nucleons, respectively. The total wave function $|\Phi\rangle$ is divide into the following two subspaces: the core part $|\Phi_C\rangle$ and the valence particle part $|\Phi_V\rangle$. It is expressed as follows:

$$|\Psi\rangle = \mathcal{A}' \{|\Phi_C\rangle|\Phi_V\rangle\}, \quad (2)$$

where the antisymmetrization $\mathcal{A}'$ represents the exchange of particles between different clusters, i.e., one from $|\Phi_C\rangle$ and another one from $|\Phi_V\rangle$. The wave functions $|\Phi_C\rangle$ and $|\Phi_V\rangle$ are individually antisymmetrized.

We use the harmonic oscillator function for describing the core. To introduce a degree of freedom for the core, we change the size parameter b of the harmonic oscillator function $\sim\exp(-r^2/2b^2)$; in the normal COSM, however, the core size is fixed. In the following discussions, we explicitly represent the dependence of the core-size parameter b as "$[b]$." The Hamiltonian for the valence nucleons is obtained by multiplying the core wave function from the left-hand side follows:

$$\begin{aligned}&\langle\Phi_C[b]|\hat{H}\,|\mathcal{A}'\{|\Phi_C[b]\rangle|\Phi_V\rangle\}\rangle \\ &\quad= \left[\sum_{i\in V} \hat{h}_i[b] + \sum_{i<j\in V} \{\hat{T}_{ij} + \hat{v}_{ij}\} + \langle H_C[b]\rangle\right] |\Phi_V\rangle. \end{aligned} \quad (3)$$

Here, $\hat{h}_i$ is a one-body operator for the ith valence nucleon and is defined as $\hat{h}_i[b] \equiv \hat{t}'_i + \hat{V}_i[b]$. $\hat{t}'_i$ is the kinetic energy operator, and $\hat{V}_i[b]$ is the folding potential constructed by taking into account the antisymmetrization between the nucleons in the core and the valence nucleon as follows:

$$\hat{V}_i[b]|\Phi_V\rangle \equiv \sum_{m\in C}\left\langle \Phi_C[b]\ |\hat{v}_{im}\,|\,\mathcal{A}'\left\{|\Phi_C[b]\rangle|\Phi_V\rangle\right\}\right\rangle. \quad (4)$$

In Eq. (3), $\hat{T}_{ij}$ is the two-body kinetic operator and is expressed as $\hat{T}_{ij} = \frac{1}{\mu}\nabla_i \cdot \nabla_j$; this results from the elimination of the center-of-mass motion. $\hat{v}_{ij}$ is the nucleon-nucleon interaction between the valence nucleons.

For the valence nucleons, we perform a type of "full-space" calculation in the COSM coordinate system [29], which is spanned by the vectors from the center-of-mass of the core to those of the valence nucleons. We use the Gaussian function for the radial part of each basis function and define a basis function for the ith valence nucleon as follows:

$$\begin{aligned} u_i(r) &= \mathcal{N} r^{l_i}\exp(-a_i r^2/2)[l_i \otimes s_i]_{j_i}\chi_i \\ &\equiv g_i(r_i)|l_i,\, j_i,\, t_i\rangle. \end{aligned} \quad (5)$$

An mth basis function $\Phi^{(m)}_{JM}$ for the valence nucleons with a total spin J is constructed by the following normal coupling scheme:

$$\begin{aligned} &\Phi^{(m)}_{JMTM_T} \\ &\quad = \mathcal{A}\left\{\left[\left[\left[u_1^{(m)}, u_2^{(m)}\right]_{J_{12}}, u_3^{(m)}\right]_{J_{123}}\cdots\right]_{JM}\cdot\chi(TM_T)\right\}, \end{aligned} \quad (6)$$

where $\chi(TM_T)$ is the total isospin function. In the case where all the valence nucleons are identical, i.e., all are either neutrons or protons, it is not necessary to calculate the isospin part explicitly. We use coefficients α_k, which originate from the recoupling of the angular momenta in the antisymmetrization of the valence nucleons, and obtain the mth basis function as follows:

$$\left|\Phi^{(m)}_{JM}\right\rangle \equiv \sum_k \alpha_k \left|\tilde{\Phi}^{(m)}_{JM:k}\right\rangle. \quad (7)$$

Here, $\tilde{\Phi}^{(m)}_{JM:k}$ is a recoupled basis function corresponding to the suffix k. In actual calculations, we retain the recoupling coefficients α_k in some cases to reduce the computational time.

Diagonalizing the Hamiltonian for the valence nucleons with the basis functions described above, we obtain eigenfunctions Ψ_{JM} as a linear combination of the basis sets:

$$\begin{aligned} \Psi_{JM} &= \sum_m c^{(m)}\Phi^{(m)}_{JM} \\ &= \sum_m c^{(m)}\mathcal{A}\{F^{(m)}(r_1, r_2, \ldots, r_N)|JMTM_T\rangle\}. \end{aligned} \quad (8)$$

Here, the radial part $F^{(m)}(r_1, r_2, \ldots)$ is the product of the Gaussian functions as follows:

$$F^{(m)}(r_1, r_2, \ldots, r_N) \equiv g_1^{(m)}(r_1)\cdot g_2^{(m)}(r_2)\cdots g_N^{(m)}(r_N). \quad (9)$$

The linear combination of $F^{(m)}(r_1, r_2, \ldots)$ is constructed by a set of different size parameters of $a_i^{(m)}$ to reproduce the radial dependence of the eigenfunction of the total system. The components of the unbound states are appropriately included in the total wave function in terms of the linear combination of the Gaussian with different size parameters.

For a small number of valence nucleons in $^{16}\mathrm{O}+XN$ systems, e.g., ^{17}O ($X = 1$) and ^{18}O ($X = 2$), we can perform "exact" calculations with a sufficiently large basis size. For example, a typical basis size for the $X = 2$ case is about 2000. However, with the increase in the number of valence nucleons, the total basis size rapidly diverges and straightforward approaches for matrix diagonalization become impractical. Therefore, we employ a stochastic variational approach [36]; this approach is discussed in the next subsection.

The energy of the core $\langle H_C[b]\rangle$ can be calculated analytically as a function of the core-size parameter b for a special case where the core wave function is the harmonic oscillator function of the lowest configuration and the Gaussian-type effective nucleon-nucleon interaction is used for the mutual interaction in the core [37].

The energy of the total system is obtained as a sum of the core $\langle H_C[b]\rangle$ and valence nucleon $\langle H_V[b]\rangle$ parts:

$$E(b) = \langle H_C[b]\rangle + \langle H_V[b]\rangle. \quad (10)$$

Here, $\langle H_V[b]\rangle$ depends on the core size b via the one-body operator $\hat{h}_i[b]$ as follows:

$$\langle H_V[b]\rangle \equiv \langle\Phi_V|\left[\sum_{i\in V}\hat{h}_i[b] + \sum_{i<j\in V}\{\hat{T}_{ij} + \hat{v}_{ij}\}\right]|\Phi_V\rangle. \quad (11)$$

The calculations of the matrix elements for the valence nucleons can be performed in a manner similar to that of the two-body matrix elements in the shell model.

B. Stochastic variational approach

In the neo-COSM formalism, we use the Gaussian for the radial part of the basis function and express the eigenfunction as a linear combination of these Gaussian basis sets. For systems with one or two valence particles, it is possible to perform an "exact" calculation by using a sufficiently large number of core-N basis functions. However, with the increase in the number of particles, the difficulty in performing such exact calculations because of the number of the basis size diverges exponentially. Therefore, we employ a stochastic variational (SV) approach to select important basis functions. The stochastic variational method (SVM) [37–39] is an efficient technique for reducing the total number of basis sets by the SV approach. A nearly identical procedure is used in the Monte-Calro shell model [40] and AMD-SSS approaches [41] for selecting the basis functions. For detailed explanations of the algorithm, please see Refs. [37–41]. Here, we use the same procedure as that used in the above-mentioned methods for selecting the basis functions.

The variational parameters in the calculation are the size parameters of the Gaussian basis function $a_i^{(m)}$ and angular momenta $j_i^{(m)}, l_i^{(m)}$ of the valence nucleons. It has been reproduced that to obtain a good energy convergence, not only the ground state but also several excited states should be taken into account in the calculation [41]. Once the eigenvalues of the Hamiltonian with i basis sets are obtained, we add an $(i+1)$th

TABLE I. Eigenvalues and components of the 0_1^+ state of ^{18}O. In the first column, SVA and Exact represent the stochastic variational approach and the calculation with sufficiently large basis sets, respectively (please see text). In the seventh column, N is the number of basis sets.

Method	E (MeV)	$R_{\rm rms}$ (fm)	$(d_{5/2})^2$	$(s_{1/2})^2$	$(d_{3/2})^2$	N
SVA	−12.180	2.635	0.838	0.101	0.038	138
"Exact"	−12.182	2.635	0.837	0.101	0.038	2100

base to the total basis function as a candidate and diagonalize the Hamiltonian with the $(i+1)$ basis sets. We calculate $\mathcal{E}$– the sum of the differences between the eigenvalues $E_n^{(i)}$ and $E_n^{(i+1)}$, defined as follows:

$$\mathcal{E} \equiv \sum_{n=1}^{n_{\max}} \left| E_n^{(i)} - E_n^{(i+1)} \right|, \tag{12}$$

where the suffix n is the label of the eigen states, e.g., $n=1$ represents the ground state. If $\mathcal{E}$ becomes greater than the convergence parameter $\mathcal{E}_0$, i.e., for $\mathcal{E} > \mathcal{E}_0$, the candidate is included in the total basis functions as the $(i+1)$th basis set. Otherwise, for $\mathcal{E} \leqslant \mathcal{E}_0$, the candidate is eliminated. In this calculation, we fix $n_{\max} = 3$ and $\mathcal{E}_0 = 10$ (keV), respectively.

An example of the calculation of the stochastic variational approach is shown in Table I. We calculated the ground state of ^{18}O (0^+) in the $^{16}\mathrm{O}+2n$ model space. The "exact" method uses the 2100 basis sets, including angular momenta up to $l=5$ $(j=11/2)$, and the results converged well for this number of basis sets. In the SV approach, the number of basis sets becomes 138 and is considerably lower than the exact value. Further, contributions of the partial angular momenta are also identical to the exact ones.

III. CALCULATED RESULTS WITH THE CLUSTER-ORBITAL SHELL MODEL

In this section, we present the calculated results for the oxygen isotopes and $N=8$ isotones for two cases: (1) fixed-b calculations, which correspond to the the normal COSM, and (2) the extended COSM, which we term neo-COSM.

A. The core-N and N-N interactions

In all our calculations, we use the Volkov No. 2 potential [42] as the effective nucleon-nucleon interaction (N-N interaction):

$$v(r) = \sum_{k=1}^{3} V_0^{(k)} \left(W_k + M_k P_M + B_k P_B - H_k P_H\right) \exp(-\rho_k r^2). \tag{13}$$

We select the Majorana parameter as $M_k = 0.58$ and fix this value in all calculations.

The folded core-N potential for the ith valence nucleon is obtained as follows:

$$\sum_{m\in C} \langle \Phi_C[b] \, | v_{im} \, | \mathcal{A}' \{ | \Phi_C[b] \rangle | \Phi_V \rangle \} \rangle \simeq \left[\hat{V}_i^d[b] + \hat{V}_i^{\rm ex}[b] + \lambda \hat{\Lambda}_i[b] \right] | \Phi_V \rangle. \tag{14}$$

In Eq. (14), $\hat{V}_i^d$ is the direct part of the folding potential; $\hat{V}_i^{\rm ex}$, the exchange part; and $\hat{\Lambda}$, the projection operator to the Pauli forbidden states. For the exchange part $\hat{V}_i^{\rm ex}$, we apply the "knock on" exchange kernel [43], which has a nonlocality and includes only the Fock term. The functional forms of $\hat{V}_i^d$ and $\hat{V}_i^{\rm ex}$ in the coordinate space are then expressed as follows:

$$\hat{V}_i^d[b](r) = \sum_k V_0^{(k)} C_k \left(\frac{\alpha_k}{\beta_k}\right)^{3/2} \times \left[(4 - 3\alpha_k b^2) + 2\alpha_k^2 b^2 r^2 \right] \exp(-\alpha_k r^2) \tag{15}$$

and

$$\hat{V}_i^{\rm ex}[b](\mathbf{r}, \mathbf{r}') = -\sum_k V_0^{(k)} C_k \left(1 + \frac{2}{b^2} \mathbf{r}\cdot\mathbf{r}'\right) \times \exp\left[-\left(\frac{1}{2b^2} + \beta_k\right)(r^2 + r'^2) + 2\beta_k \mathbf{r}\cdot\mathbf{r}' \right], \tag{16}$$

where $\alpha_k \equiv 16\beta_k/(16 + 15b^2\beta_k)$, $\beta_k = 1/(1+2b^2\rho_k)$, and $C_k \equiv 4W_k - M_k + 2B_k - 2H_k$.

Additionally, we introduce an effective LS potential to reproduce the energy splitting of the low-lying positive parity states $5/2^+$ and $3/2^+$ of ^{17}O. The functional form of the LS potential is as follows:

$$V_{ls}[b](r) = \mathbf{L}\cdot\mathbf{S} V_{ls}^0 f\left(\frac{r}{b}\right). \tag{17}$$

Here, $f(x) \equiv (2x^2 - 1)\exp(-x^2)$ and V_{ls}^0 is the strength parameter of the LS interaction determined by fitting the LS splitting of the lowest positive parity states $5/2^+$ and $3/2^+$ as $V_{ls}^0 = 97.5$ (MeV).

To eliminate the Pauli forbidden states in the core, we apply the orthogonality condition model (OCM) [44]. As shown in many studies employing OCM [31–34], the conventional method to eliminate the forbidden states involves the multiplication of an arbitrary constant λ to the projection operator $\hat{\Lambda}$ of the Pauli forbidden state $|F.S.\rangle$ and to consider λ as a sufficiently large number in the diagonalization of the Hamiltonian.

By considering all theses terms together, the Hamiltonian for the ith valence particle $\hat{h}_i$ becomes as follows:

$$\hat{h}_i[b] = \hat{t}_i + \hat{V}_i^d[b] + \hat{V}_i^{\rm ex}[b] + \hat{V}_{ls}[b] + \lambda\hat{\Lambda}_i[b]. \tag{18}$$

The energies of the three lowest states $5/2^+$, $1/2^+$, and $3/2^+$ are obtained as -4.175, -3.272, and $0.962 - i0.070$ (MeV), respectively. The imaginary part in the energy of the $3/2^+$ state represents a half of the total decay width, i.e., $\Gamma = 0.14$ (MeV). The results are shown in Fig. 1.

In this calculation, for the resonant state $3/2^+$, we use CSM [9–11] with the rotational angle $\theta = 10$ (degree). In CSM,

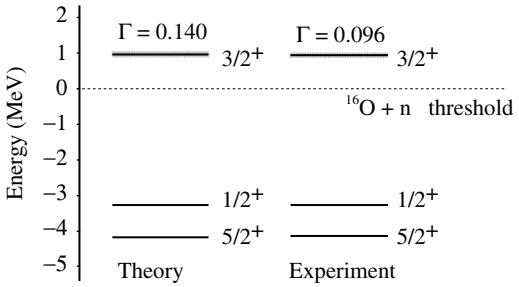

FIG. 1. Calculated levels of ^{17}O and experimental data [45].

the resonant wave functions become L^2 integrable, and the eigenvalues are obtained as complex numbers in which the real and imaginary parts correspond to the resonant energy and a half of the total decay width, respectively.

The Coulomb interaction between the core and a valence proton is also microscopically constructed by folding the core wave function. As mentioned in Ref. [43], the exchange part of the folded core-p Coulomb potential contributes as an attractive force. Hence, the energy of the ground state of ^{17}F ($^{16}\mathrm{O} + p$ is calculated as -0.846 (MeV); this energy value exceeds that obtained by experiment, -0.600 (MeV).

For the interaction among valence nucleons, we modify the exchange parameters H_k and B_k in the Volkov interaction as $H_k = B_k = 0.069$ to fit the energy of the ^{18}O ground state. The calculated levels and experimental data are shown in Fig. 2. In the calculations, we use the "exact" method, which is described in Sec. II B, and the resonant states of ^{18}O are calculated by CSM with the rotational angle $\theta = 10$ (degree), which is identical to the calculation for the ^{17}O case.

Because we use a core-plus-two valence nucleons model, the components of particle-hole excitations in the core are not included in the calculation. Hence, the observed 0_2^+ (3.63 MeV), 2_3^+ (5.25 MeV), and 4_2^+ (7.12 MeV) levels are not described in our model space because they are dominantly $4p$-$2h$ states. Further, the calculated second 0^+ state corresponds to the 0_3^+ (5.34 MeV) level, which has a large $(s_{1/2})^2$ component.

Next, we calculate the core energy microscopically. To maintain the consistency between the description of the core and the core-N potential, we use the same lowest configuration of the harmonic oscillator wave function. However, as mentioned in Ref. [37], the saturation property of ^{16}O cannot be reproduced by only using a two-body effective interaction. Hence, we introduce an effective three-body

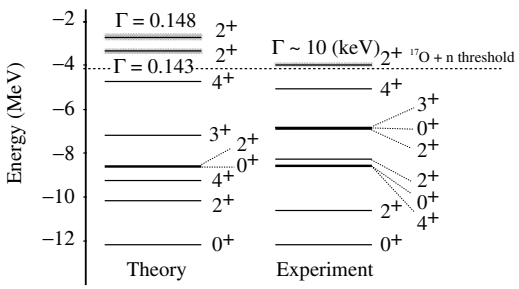

FIG. 2. Calculated levels of ^{18}O and experimental data [46].

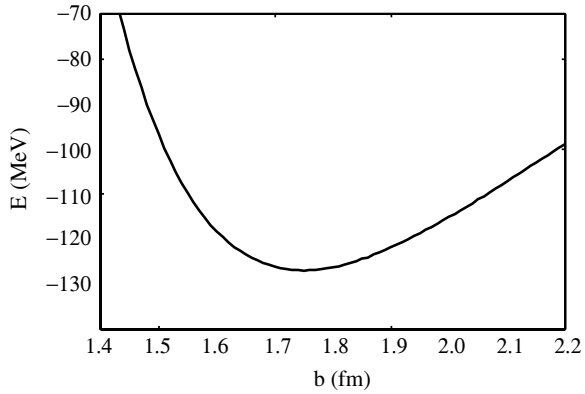

FIG. 3. Calculated energy of ^{16}O obtained by using the Volkov No. 2 interaction with the effective three-body repulsive force.

repulsive potential $V_{ijk}^{(3)}$ to the core Hamiltonian, which is identical to the δ-type interaction in Ref. [37]:

$$V_{ijk}^{(3)} = v^{(3)}\delta(\mathbf{r}_i - \mathbf{r}_j)\,\delta(\mathbf{r}_j - \mathbf{r}_k). \tag{19}$$

The analytical form of the energy of ^{16}O in the function of the core-size parameter b is then expressed as follows [37]:

$$E(b) = \frac{69}{4}\hbar\omega + \sum_k v_k \beta_k^{3/2}\left[\left(\frac{31}{4} - \frac{3}{2}\beta_k + \frac{15}{4}\beta_k^2\right) \times \left(X_k^d + X_k^{\mathrm{ex}}\right) + 6\beta_k\left(X_k^d - X_k^{\mathrm{ex}}\right)\right] + e^2\frac{83}{4} \times \left(\frac{2}{\pi b^2}\right)^{1/2} + 16 \times \frac{29}{9}\left(\frac{1}{3\pi b^4}\right)^{3/2} v^{(3)}, \tag{20}$$

where $X_k^d = 8W_k + 4B_k - 4H_k - 2M_k$ and $X_k^{\mathrm{ex}} = 8M_k + 4H_k - 4B_k - 2W_k$.

In the calculation of the core energy, we modify the strength of the repulsive part in the Volkov interaction as $v_2 = 46.1$ (MeV) to avoid a counting the repulsive force two times because of the introduction of the three-body repulsive potential in the core Hamiltonian. We select the strength of the effective three-body potential as $v^{(3)} = 3900$ (MeV fm^6) to reproduce the energy of ^{16}O as $E/A = 7.93$ (MeV).

The calculated energy curve is shown in Fig. 3. The rms radius of ^{16}O is obtained as $R_{\mathrm{rms}} = 2.57$ (fm). As seen in Fig. 3, the energy curve becomes flatter around the minimum point. This is an important feature that enable the b dependence in total-energy calculation with different number of valence nucleons.

B. Results with the fixed-b calculations

First, we calculate the binding energies and the rms radii of the oxygen isotopes and $N = 8$ isotones with a fixed core-size parameter $b = 1.723$ (fm). The fixed core size is determined so as to reproduce the rms radius of $^{16}\mathrm{O}$ – $R_{\mathrm{rms}} = 2.53$ (fm). In this calculation, the basis sets are selected by using the stochastic variational approach, which is shown in Sec. II B.

The energies of the oxygen isotopes and $N = 8$ isotones are shown in the left- and right-half regions of Fig. 4, respectively. The calculated binding energies agree with the

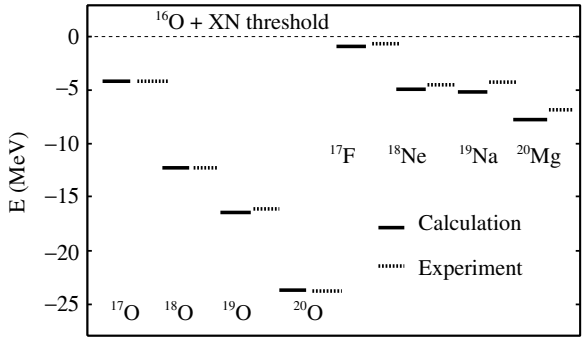

FIG. 4. Calculated energies with respect to the ^{16}O + XN threshold and the experimental values [45,46] for the oxygen isotopes and $N = 8$ isotones.

experimental data [45,46]. For the $N = 8$ isotones, although the total energies with respect to the ^{16}O + Xp threshold exceed the binding energies, the one-proton separation energies of ^{18}Ne and ^{20}Mg almost agree with the experimental values. The calculated one-proton separation energies are $S_p(^{18}\text{Ne}) = 4.016$ (MeV) and $S_p(^{20}\text{Mg}) = 2.657$ (MeV), and the experimental values are $S_p(^{18}\text{Ne}) = 3.922$ (MeV) and $S_p(^{20}\text{Mg}) = 2.650$ (MeV).

We calculated the rms radii for the isotopes and isotones. In comparison to the good agreement between the binding energies, the calculated rms radii show some difference from the experimental values. For the oxygen isotopes, the calculated rms radii agree with the experiments within the error bars as shown in Fig. 5(a). In contrast, for the $N = 8$ isotones, the calculated radii are systematically smaller than the experimental values, see Fig. 5(b). Moreover, for oxygen isotopes and $N = 8$ isotones, there is no significant change in the radii when the change in mass number A changes from 17 to 18 and from 18 to 20.

In our COSM calculation, the asymptotic behavior of the valence nucleons is appropriately taken into account in terms of the linear combination of the Gaussian basis sets, even for fixed

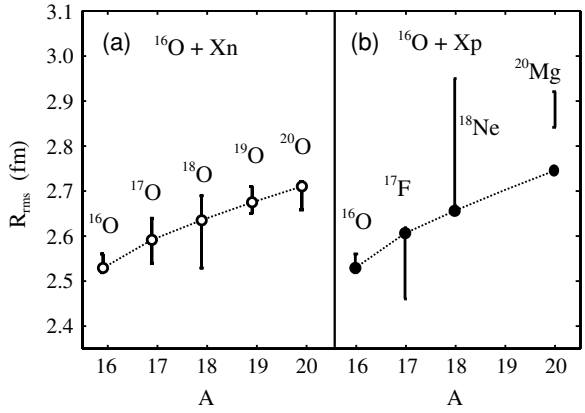

FIG. 5. Calculated rms radii for (a)^{16}O + Xn and (b)^{16}O + Xp systems with a fixed b parameter and the experimental values [2]. Open and solid circles indicate calculated values, and lines with error bars indicate the experimental values. The dotted lines are drawn as eye guides.

b value. Nevertheless, the abrupt increase in the radii of ^{18}Ne or ^{20}Mg is not reproduced only by the asymptotic behavior of the wave function. This indicates that other mechanisms must be sought to explain this behavior of the radii. Therefore, we extended the COSM formalism by introducing the dynamics of the core.

C. Results with an extended COSM: Neo-COSM

To consider the dynamics of the core, we first introduce a degree of freedom for the core-size parameter b. Because of both the energy of the core and the core-N potential are constructed from the same core density, the effect of the change in the core on the total system can be discussed microscopically through the change in the core-size parameter. We refer to this approach as neo-COSM.

In the fixed-b calculation, the binding energies of the ^{16}O + XN systems are almost reproduced. However, the rms radii for $N = 8$ isotones were smaller than the experimental values, whereas those for the oxygen isotopes agreed with the experimental values. The main difference between the $N = 8$ isotones and the oxygen isotopes is the presence of the Coulomb interaction. If a larger value of the core-size parameter is adopted in an isotone because of the presence of the Coulomb interaction, the rms radius of the isotone becomes larger than that of the isotope that has the same mass number. Further, the optimum value of the core-size parameter depends on the number of valence nucleons because the energy of the total system is determined by the sum of the energies of the core and valence nucleons. The energy of the valence nucleon part is determined by the configuration mixing of the single-particle states, which also depends on the core size via the core-N potential. Therefore, we expect that the optimum point of the core-size parameter b exhibits isotope and isotone dependence. This will be a key mechanism for explaining the abrupt increase in the rms radii in this mass region.

First, we calculate the energies of ^{17}O (^{16}O + n) and ^{17}F (^{16}O + p) by changing the core-size parameter b. The energies are calculated for the ground state and the first excited states $5/2^+(l = 2)$ and $1/2^+(l = 0)$. The results are shown in Fig. 6.

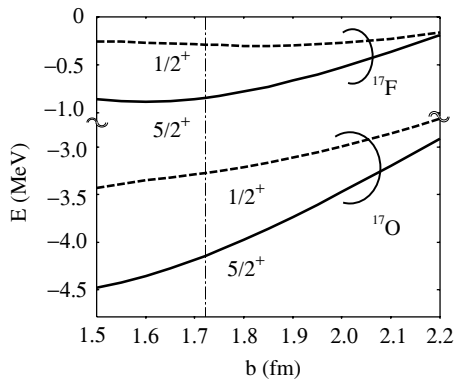

FIG. 6. The change in the energy of the $5/2^+$ and $1/2^+$ state for ^{17}O and ^{17}F, respectively. The dash-dotted line shows the fixed b value; $b = 1.723$ (fm).

For ^{17}O, the energy curves of the $5/2^+$ and $1/2^+$ states ascend monotonically with the increase in b in the range of 1.5 to 2.2 (fm). Despite this property of the energy curves, the total systems do not have an extremely small b value because of the saturation properties of the ^{16}O core as shown in Fig. 3.

However, for ^{17}F, the energy of the $1/2^+$ state is insensitive to the change in b, although the behavior of its $5/2^+$ state is almost identical to that of the ^{17}O state. We consider that such this discrepancy between ^{17}O and ^{17}F, in terms of the relation between $1/2^+$ and the change in b, is closely related to the Thomas-Ehrman shift. The Thomas-Ehrman shift can be simply explained as follows. When a centrifugal barrier is present, wave functions with nonzero angular momenta are localized inside its region, and they experience Coulomb repulsion. Hence, the binding energy of the $5/2^+$ state of ^{17}F becomes smaller than that of ^{17}O. In contrast, the s wave does not have a centrifugal barrier, and the wave function is not localized. In this case, the energy loss because of Coulomb repulsion becomes smaller than that for states with higher angular momenta. Consequently, the energy difference between the $5/2^+$ and $1/2^+$ states of ^{17}F becomes smaller than that of ^{17}O.

In addition, because the $1/2^+$ state of ^{17}F is not localized because of the absence of the centrifugal barrier, its energy becomes insensitive to the change in b; see Fig. 6. The difference in the behaviors of the $5/2^+$ and $1/2^+$ states because of changed in the core-size parameter will be a key mechanism for creating the isotope and isotone dependence in the neo-COSM calculation.

We calculate the total energies of the $5/2^+$ state of ^{17}F and ^{17}O. The optimum values of the core-size parameter are determined from the minimum point of the energy of the total system, as shown in Eq. (10). For the $5/2^+$ ground state, the optimum b values for ^{17}O and ^{17}F are identical, that is, obtained as $b = 1.76$ (fm). The change in the energies in the case of the fixed-b calculation is small, that is, less than 0.2 MeV. The rms radii are obtained as $R_{\rm rms} = 2.62$ and 2.64 (fm) for ^{17}O and ^{17}F, respectively. These values are larger than those obtained by fixed-b calculations in 0.02 (fm). In the calculation for the $5/2^+$ state, the values for ^{17}O and ^{17}F are not very different each other because other states, e.g., the $1/2^+$ state, do not contribute to the calculation of the total energy.

Next, we perform calculations for ^{18}O (^{16}O+2n) and ^{18}Ne (^{16}O + 2p). In this case, the number of valence nucleons is two; therefore, the eigenfunctions become a linear combination of the core-N basis functions with different angular momenta. Hence, the difference in the b dependence of the neutron and proton cases will be apparent in the total wave function.

Results for the calculations of the energies of the 0^+ ground states and the rms radii of ^{18}O and ^{18}Ne are shown in Table II. The optimum value of b is 1.74 (fm) for both ^{18}O and ^{18}Ne. Because of the change in the adopted b from the fixed value, the ground-state energies become smaller than those obtained by the fixed-b calculation. The calculated rms radii of ^{18}O and ^{18}Ne are $R_{\rm rms} = 2.65$ (fm) and 2.68 (fm), respectively. Even though the adopted-b values in the neo-COSM calculations for ^{18}O and ^{18}Ne are identical, the radii obtained from the fixed-b and neo-COSM calculations are different.

TABLE II. The calculated energies and rms radii from fixed-b and neo-COSM calculations.

		E (MeV)	$R_{\rm rms}$ (fm)	$(d_{5/2})^2$	$(s_{1/2})^2$
^{18}O:	Fixed-b	−12.18	2.64	0.836	0.103
	Neo-COSM	−12.00	2.65	0.832	0.106
	Expt. [2,46]	−12.19	2.61 ± 0.08	—	—
^{18}Ne:	Fixed-b	−4.94	2.66	0.824	0.115
	Neo-COSM	−4.68	2.68	0.812	0.125
	Expt. [2,46]	−4.52	2.81 ± 0.14	—	—

To investigate the mechanism that causes this difference, we expand the wave function of the 0^+ ground state with the core-N components as $|0^+\rangle = c_1|(d_{5/2})^2\rangle + c_2|(s_{1/2})^2\rangle + \cdots$. Here, each component, for example $(d_{5/2})^2$, indicates that two valence nucleons have an angular momentum $l = 2$ ($j = 5/2$). In the shell-model picture, $d_{5/2}$ corresponds to the sum of all states with an angular momentum $l = 2$ ($j = 5/2$), i.e., $0d_{5/2}, 1d_{5/2}, 2d_{5/2}, \ldots$. In our COSM calculation, all these components are contained in the linear combination of the Gaussian basis functions.

The calculated weights c_i^2 are listed in the fourth and fifth columns of Table II. In ^{18}O, there is no significant difference between the results of the neo-COSM and fixed-b calculations. The weights of $(d_{5/2})^2$ of the neo-COSM and fixed-b calculations are obtained as 0.832 and 0.836, respectively. The difference between the two approaches is only 0.004. Similarly, the weight of $(s_{1/2})^2$ are obtained as 0.106 and 0.103, and the difference is 0.003. This shows that in ^{18}O, the configuration of the 0^+ state does not change in the fixed-b and neo-COSM calculations.

However, in ^{18}Ne, the difference between the components $(d_{5/2})^2$ and $(s_{1/2})^2$ in the fixed-b and neo-COSM calculations is not as small as that in ^{18}O. The $(d_{5/2})^2$ component decreases from 0.824 to 0.812, and the $(s_{1/2})^2$ component increases from 0.115 to 0.125. A remarkable feature is the increase in the s-wave component. The difference between the two values obtained by two approaches is 0.010, which is over three times greater than that in ^{18}O. We consider the following cause for the suppression of $(d_{5/2})^2$ and the enhancement of $(s_{1/2})^2$ in the neo-COSM calculation. As shown in Fig. 6 for the ^{17}F case, the effects on the components $(s_{1/2})^2$ and $(d_{5/2})^2$ are different, even though the adopted b parameter is similar to that in ^{18}O. The s-wave component is insensitive to the change in the core-size parameter. Therefore, when a larger b value is adopted, the $(s_{1/2})^2$ component is enhanced, whereas the $(d_{5/2})^2$ component loses more energy as b increase. Because the s-wave component has a broader radius than the other partial waves, the rms radius of ^{18}Ne obtained by the neo-COSM calculation becomes larger than that by the fixed-b calculation.

Finally, we perform the neo-COSM calculation for ^{16}O + XN systems up to $X = 4$. The calculated rms radii and their comparison with the experimental values are shown in Fig. 7(a) for the oxygen isotopes (^{16}O + Xn systems) and in Fig. 7(b) for the $N = 8$ isotones (^{16}O + Xp systems). By comparing the result of oxygen isotopes in Figs. 5(a)

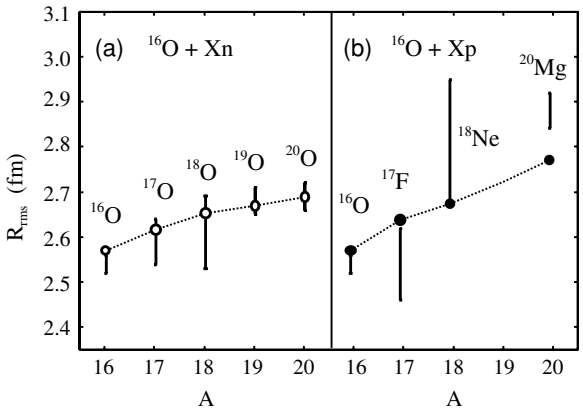

FIG. 7. Neo-COSM-calculated rms radii for (a)^{16}O + Xn and (b)^{16}O + Xp systems, and the experimental values [2]. Open and solid circles indicated calculated values and the lines with error bars indicate the experimental values. The dotted lines are drawn as eye guides.

and 7(a), we find that the changes in the rms radii obtained by the neo-COSM calculation with the increase in the number of valence neutrons becomes smaller than those obtained by the fixed-b calculation. However, by comparing Figs. 5(b) and 7(b) for the $N = 8$ isotone, the increase in the rms radii obtained by the neo-COSM calculation become sizable at ^{20}Mg, whereas there is no rapid increase in the fixed-b calculation values. This is because of the difference in the adopted-b values in the neo-COSM calculation for the isotopes and isotones. The adopted b values and radii are shown in Table III. For the oxygen isotopes, the adopted b for the neo-COSM calculation reduces with the increase in the valence neutron number. In contrast, for the $N = 8$ isotones, the adopted-b values remain the same in ^{18}Ne and ^{20}Mg, as shown in Table III. Therefore, the rms radius of ^{20}Mg becomes considerably larger than that of ^{20}O, and the result improved qualitatively, thereby enabling the reproduction of the experiment.

We also calculate the difference in the rms radii, R_D of the $N = 8$ isotones and the oxygen isotopes, which is defined as follows:

$$R_D \equiv R_{\rm rms}(^{16}{\rm O} + Xp) - R_{\rm rms}(^{16}{\rm O} + Xn). \qquad (21)$$

In the systems with $X = 1$ and 2, R_D values obtained are identical for both fixed-b and neo-COSM calculations. However, for $X = 4$, the difference in the radii is obtained as $R_D = 0.08$ (fm) in the neo-COSM calculation, whereas the fixed-b calculation yields $R_{\rm rms} = 0.04$ (fm); see Table IV. Therefore, it is shown that the neo-COSM approach qualitatively improves the rms radii of the ^{16}O + XN systems up to $X = 4$.

TABLE III. $R_{\rm rms}$ and adopted b values obtained by the neo-COSM calculations. All values are in fm.

	^{16}O	^{17}O	^{18}O	^{19}O	^{20}O	^{17}F	^{18}Ne	^{20}Mg
$R_{\rm rms}$	2.57	2.62	2.65	2.67	2.69	2.64	2.68	2.77
b	1.75	1.76	1.74	1.72	1.71	1.76	1.74	1.74

TABLE IV. R_D for the fixed-b and neo-COSM calculations. All values are in fm. For the definition of R_D, please see the text.

	R_D: ^{17}F-^{17}O	^{18}Ne-^{18}O	^{20}Mg-^{20}O
Fixed b	0.02	0.02	0.04
Neo-COSM	0.02	0.03	0.08

IV. SUMMARY

We studied oxygen isotopes and $N = 8$ isotones by an extended cluster-orbital shell model referred to as neo-COSM. The calculated rms radii of the isotones and isotopes improved qualitatively in comparison to the fixed-b calculation.

An important feature of the neo-COSM calculation is that the motion of the valence nucleons is solved as a linear combination of the Gaussian basis functions by using the stochastic variational (SV) approach. Because of the characteristics of the COSM formalism, the correlations among the valence nucleons can be described by solving the system. Simultaneously, the asymptotic behavior of the wave functions are appropriately described by the linear combination of the Gaussian. Therefore, if the system has a halo structure, the eigenfunction is obtained as COSM with the SV approach.

Another important feature of the neo-COSM is that the total system is separated into two subspaces—the core part and the valence nucleons part. Thus far, we have limited our study by considering that the configuration of the core wave function is the lowest in the harmonic oscillator; however, the dynamics of the core can be taken into account through the change in the core-size parameter b. The energy of the core and the core-N folding potential changed with the change in b. Hence, different nuclei have different b, which are determined by considering the minimum point of the energy of the total system.

The mechanism of the qualitative improvement in the rms radius of ^{20}Mg obtained by the neo-COSM calculation will be a key to solving the problem of the large radii of drip-line nuclei ^{23}O and ^{24}O. In the lowest configuration of ^{22}O, the $0d_{5/2}$ orbit is entirely occupied. The change in the core-size parameter b mainly affects on the $1s_{1/2}$ state. The energy dependence of the $1s_{1/2}$ state is smaller than that of the $0d_{5/2}$ state. In a manner identical to the mechanism in the $N = 8$ isotones, the weight of the $1s_{1/2}$ state increases with the core-size parameter b. Therefore, we can expect that the minimum point of the total energy in the change of the core b parameter becomes a larger value, and the rms radii of ^{23}O and ^{24}O abruptly become large from ^{22}O.

In this calculation, we consider only the change in the core-size parameter b to introduce the dynamics of the core. In future studies, different types of degrees of freedom should be taken into account in the neo-COSM calculation. We showed that the COSM formalism is a useful tool for the study of weakly bound nuclei. Its application to heavier nuclei is an important challenge, and it will be worthwhile to study the role of the correlations of valence nucleons in the COSM formalism.

ACKNOWLEDGMENTS

The authors thank the members of the nuclear theory group at Hokkaido University for their interest and discussions. The authors also thank Professor Motobayashi and Dr. Myo for useful discussion. This study was partially carried out as a Research Project for the Study of Unstable Nuclei from Nuclear Cluster Aspects sponsored by the Institute of Physical and Chemical Research (RIKEN).

[1] A. Ozawa *et al*., Nucl. Phys. **A691**, 599 (2001).
[2] A. Ozawa, T. Suzuki, and I. Tanihata, Nucl. Phys. **A693**, 32 (2001).
[3] R. Kanungo *et al*., Phys. Rev. Lett. **88**, 142502 (2002).
[4] R. Kanungo, I. Tanihata, and A. Ozawa, Phys. Lett. **B512**, 261 (2001).
[5] O. Tarasov *et al*., Phys. Lett. **B409**, 64 (1997).
[6] H. Sakurai *et al*., Phys. Lett. **B448**, 180 (1999).
[7] H. Y. Zhang *et al*., Nucl. Phys. **A707**, 303 (2002).
[8] E. Khan *et al*., Phys. Lett. **B490**, 45 (2000).
[9] J. Aguilar and J. M. Combes, Commun. Math. Phys. **22**, 269 (1971).
[10] E. Balslev and J. M. Combes, Commun. Math. Phys. **22**, 280 (1971).
[11] Y. K. Ho, Phys. Rep. **99**, 1 (1983).
[12] B. A. Brown, Prog. Part. Nucl. Phys. **47**, 517 (2001).
[13] T. Otsuka, M. Honma, T. Mizusaki, N. Shimizu, and Y. Utsuno, Prog. Part. Nucl. Phys. **47**, 319 (2001).
[14] E. Caurier, F. Nowacki, and A. Poves, Nucl. Phys. **A742**, 14 (2004).
[15] U. Fano, Phys. Rev. **124**, 1866 (1961).
[16] C. Mahaux and H. A. Weidenmüller, *Shell-Model Approach to Nuclear Reactions* (North-Holland, Amsterdam, 1969).
[17] J. Okołowicz, M. Płoszajczak, and I. Rotter, Phys. Rep. **374**, 271 (2003).
[18] K. Bennaceur, F. Nowacki, J. Okołowicz, and M. Płoszajczak, Nucl. Phys. **A671**, 203 (2000).
[19] N. Michel, W. Nazarewicz, M. Płoszajczak, and K. Bennaceur, Phys. Rev. Lett. **89**, 042502 (2002).
[20] N. Michel, W. Nazarewicz, M. Płoszajczak, and J. Okołowicz, Phys. Rev. C **67**, 054311 (2003).
[21] N. Michel, W. Nazarewicz, and M. Płoszajczak, Phys. Rev. C **70**, 064313 (2004).
[22] R. Id Betan, R. J. Liotta, N. Sandulescu, and T. Vertse, Phys. Rev. Lett. **89**, 042501 (2002).
[23] R. Id Betan, R. J. Liotta, N. Sandulescu, and T. Vertse, Phys. Rev. C **67**, 014322 (2003).
[24] R. Id Betan, R. J. Liotta, N. Sandulescu, and T. Vertse, Phys. Lett. **B584**, 48 (2004).
[25] G. Hagen, M. Hjorth-Jensen, and J. S. Vaagen, Phys. Rev. C **71**, 044314 (2005).
[26] G. Gamow, Z. Phys. **51**, 204 (1928); **52**, 510 (1929).
[27] T. Berggren and P. Lind, Phys. Rev. C **47**, 768 (1992).
[28] T. Berggren, Nucl. Phys. **A109**, 265 (1968).
[29] Y. Suzuki and K. Ikeda, Phys. Rev. C **38**, 410 (1988).
[30] Y. Tosaka, Y. Suzuki, and K. Ikeda, Prog. Theor. Phys. **88**, 1140 (1990).
[31] S. Aoyama, S. Mukai, K. Katō, and K. Ikeda, Prog. Theor. Phys. **93**, 99 (1995).
[32] T. Myo, S. Aoyama, K. Katō, and K. Ikeda, Prog. Theor. Phys. **108**, 133 (2002).
[33] T. Myo, K. Katō, and K. Ikeda, Prog. Theor. Phys. **113**, 763 (2005).
[34] T. Myo, K. Katō, S. Aoyama, and K. Ikeda, Phys. Rev. C **63**, 054313 (2001).
[35] H. Masui, T. Myo, K. Katō, and K. Ikeda, Eur. Phys. J. A **25**, Supplement 1, 505 (2005).
[36] V. I. Kukulin and V. M. Krasnopol'sky, J. Phys. G **3**, 795 (1977).
[37] T. Ando, K. Ikeda, and A. Tohsaki-Suzuki, Prog. Theor. Phys. **64**, 1608 (1980).
[38] K. Varga, Y. Suzuki, and R. G. Lovas, Nucl. Phys. **A571**, 447 (1994).
[39] K. Varga and Y. Suzuki, Phys. Rev. C **52**, 2885 (1995).
[40] T. Otsuka, M. Honma, and T. Mizusaki, Phys. Rev. Lett. **81**, 1588 (1998) and references therein.
[41] N. Itagaki, A. Kobayakawa, and S. Aoyama, Phys. Rev. C **68**, 54302 (2003).
[42] A. B. Volkov, Nucl. Phys. **74**, 33 (1965).
[43] T. Kaneko, M. LeMere, and Y. C. Tang, Phys. Rev. C **44**, 1588 (1991).
[44] S. Saito, Prog. Theor. Phys. Suppl. **62**, 11 (1977).
[45] F. Ajzenberg-Selove, Nucl. Phys. **A460**, 1 (1986).
[46] F. Ajzenberg-Selove, Nucl. Phys. **A475**, 1 (1987).